Electronic Supplementary Material (ESI) for CrystEngComm.

A series of POM-based compounds by tunning coordination groups and spacers of ligands: electrocatalytic, capacitive and photoelectrocatalytic properties

Chenxi Sun, Jun Ying,* Liang Jin, Aixiang Tian, Xiuli Wang*

Table S1. Selected bond lengths (Å) and angles (°) of compounds **1–7**.

Compound **1**

Co(2)-O(1)^{1}	2.125(5)	Co(1)-O(25)	2.148(6)
Co(2)-N(4)	2.097(7)	Co(1)-O(25)	2.148(6))
Co(2)-N(1)	2.154(17)	Co(1)-N(6)	2.154(8)
Co(2)-N(4)	2.097(7)	Co(1)-N(12)	2.130(7)
O(1)-Co(2)-O(31)	76.2(2)	O(1)^{1}-Co(1)-O(25)	174.8(2)
N(4)-Co(2)-O(1)	91.4(2)	O(1)^{1}-Co(1)-N(6)	102.3(2)
N(4)-Co(2)-O(1)	163.3(3)	O(1)^{1}-Co(1)-N(12)	84.6(2)

Symmetry codes for **1**: #1 1/2-X, -1/2+Y, 1/2-Z

Compound **2**

Cu(1)-N(8)^{2}	2.02(3)	Cu(1)-N(8)	2.02(3)
Cu(1)-O(35)^{2}	2.338(19)	Cu(1)-O(35)	2.338(19)
Cu(1)-N(1)^{2}	1.99(2)	Cu(1)-N(1)	1.99(2)
N(1)-Cu(1)-N(8)^{2}	90.6(11)	N(1)^{2}-Cu(1)-O(35)	89.5(10)
N(8)-Cu(1)-O(35)	88.7(10)	N(8)-Cu(1)-O(35)^{2}	91.3(10)
N(8)^{2}-Cu(1)-O(35)^{2}	88.7(10)	N(1)-Cu(1)-N(8)^{2}	90.6(11)
N(1)^{2}-Cu(1)-N(8)	90.6(11)	N(1)^{2}-Cu(1)-N(8)^{2}	89.4(11)

Symmetry codes for **2**: #1 -X, 1-Y, 1-Z; #2 1-X, 1-Y,1 -Z

Compound **3**

Cu(1)-O(1)	1.968(7)	Cu(1)-N(8)^{1}	1.979(9)
Cu(1)-N(4)	1.984(9)	Cu(2)-N(10)	2.189(10)
Cu(1)-N(12)	2.218(11)	Cu(2)-O(4)	1.957(7)
Cu(3)-O(46)	2.00(3)	Cu(3)-N(2)	2.183(15)
O(1)-Cu(1)-N(4)	92.3(4)	O(1)-Cu(2)-O(38)	76.5(3)
O(1)-Cu(1)-N(12)	91.2(3)	O(1)-Cu(2)-N(10)	90.3(3)
N(8)^{1}-Cu(1)-O(30)	90.1(4)	O(4)-Cu(2)-O(1)	168.6(3)

Symmetry codes for **3**: #1 1/2-X, +Y, -1/2+Z; #2 1/2+X, -Y, +Z

Compound **4**

Co(1)-O(1)^{1}	2.132(3)	Co(1)-O(1)	2.132(3)
Co(1)-N(1)^{1}	2.130(4)	Co(1)-N(1)	2.130(4)
Co(1)-N(8)^{1}	2.102(4)	Co(1)-N(8)	2.102(4)
O(1)-Co(1)-O(1)^{1}	180.0	N(1)^{1}-Co(1)-O(1)	93.46(13)
N(1)-Co(1)-O(1)	86.54(13)	N(1)-Co(1)-O(1)^{1}	93.46(13)
N(8)-Co(1)-O(1)	89.11(13)	N(8)-Co(1)-N(1)	88.32(15)
N(8)^{1}-Co(1)-N(1)^{1}	89.12(13)	N(8)-Co(1)-N(1)^{1}	91.68(15)

Symmetry codes for **4**: #1 1-X, 1-Y, 1-Z

Compound **5**

Co(1)-N(1)	2.039(3)	Co(2)-O(3W)^{4}	2.135(3)
Co(2)-O(3W)	2.135(3)	Co(2)-O(2W)	2.119(3)
Co(2)-O(2W)^{4}	2.119(3)	Co(2)-N(6)	2.111(3)
N(1)-Co(1)-O(1)	94.59(11)	N(1)-Co(1)-O(1W)	173.55(13)
N(1)-Co(1)-N(4)^{3}	98.95(12)	N(1)-Co(1)-O(7)^{2}	88.05(11)
N(6)-Co(2)-O(3W)	89.78(12)	N(6)-Co(2)-O(2W)^{4}	87.23(12)
O(2W)-Co(2)-O(3W)	92.06(11)	N(6)^{4}-Co(2)-O(2W)^{4}	92.77(12)

Symmetry codes for **5**: #1 2-X, 2-Y,1-Z; #2 +X, 3/2-Y, -1/2+Z; #3 +X, 1+Y, +Z; #4 -X, -Y, -Z

Compound **6**

Co(2)-O(8)	2.093(4)	Co(2)-O(16)	2.059(4)
Co(2)-N(1)	2.126(5)	Co(2)-O(33)	2.109(4)
Co(1)-N(3)	2.094(5)	Co(1)-O(7)	2.091(4)
Co(2)-O(11)	2.092(5)	Co(1)-O(5)	2.084(4)
O(8)-Co(2)-N(1)	91.12(19)	O(11)-Co(2)-O(17)^{5}	176.85(17)
O(11)-Co(2)-N(1)	91.50(19)	O(16)-Co(2)-N(1)	90.42(19)
O(7)-Co(1)-N(3)	88.54(17)	O(7)-Co(1)-O(21)	89.72(16)

Symmetry codes for **6**: #1 1-X, 3-Y, 1-Z; #2 X, -Y, -Z; #3 1-X, 2-Y, 1-Z; #4 1+X, 1+Y, +Z

Compound **7**

Cu(1)-O(20)	2.204(3)	Cu(1)-O(26)	1.964(3)
Cu(1)-N(1)^{3}	2.000(3)	Cu(1)-N(7)^{3}	2.036(4)
Cu(1)-N(4)	1.974(4)	N(1)-N(4)	1.376(5)
N(1)^{3}-Cu(1)-O(20)	109.31(13)	N(1)^{3}-Cu(1)-N(7)^{3}	79.22(15)
O(6)^{2}-Cr(2)-O(6)	180.0	O(6)-Cr(2)-O(12)	95.85(13)

O(1)-Cr(1)-O(8)	83.88(18)	O(8)[1]-Cr(1)-O(4)	96.23(13)
O(8)-Cr(1)-O(4)	83.77(13)	N(4)-Cu(1)-O(20)	94.88(15)

Symmetry codes for **7**: #1 -1-X, 1-Y, -Z; #2 -X, 2-Y, -1-Z; #3 -X, 2-Y, -Z

Table. S2. Comparison of the specific capacitance values of **1**–GCE and **4**–GCE with the reported POM-based electrodes

Electrodes	**Specific capacitance (F g^{-1})**	**Current densities (A g^{-1})**	**Ref.**
1–GCE	212	1	This work
4–GCE	202	1	This work
$H[Cu_2(4\text{-}Hdpye)_2(PMo_{12}O_{40})(H_2O)_4]\cdot 2H_2O$	151.9	1	S1
$(H_2bipy)_2[(C_6H_5PO_3)_2Mo_5O_{15}]\cdot 2H_2O$	35.3	2	S2
$H_2[Cu^I{}_2(bipy)_{2.5}(C_6H_5PO_3)_2Mo_5O_{15}]\cdot 2H_2O$	86.8	2	S2
C-PDA/PMA-1:1	101	1	S3
$H_3PW^{VI}{}_{12}O_{40}\cdot(BPE)_{2.5}\cdot 3H_2O$	49.2	2	S4

[S1] Q. Q. Liu, X. L. Wang, H. Y. Lin, Z. H. Chang, Y. C. Zhang, Y. Tian, J. J. Lu and L. Yu, *Dalton Trans.*, 2021, **50**, 9450.

[S2] B. R. Lu, S. B. Li, J. Pang, L. Zhang, J. J. Xin, Y. Chen, X. G. Tan, *Inorg. Chem.,* 2020, **59**, 1702.

[S3] Z. J. Zhang, Q. Z. Song, W. X. He, P. Liu, Y. H. Xiao, J. Y. Liang and X. Y. Chen, *Dalton Trans.*, 2019, 48, 17321.

[S4] C. L. Wang, S. Rong, Y. Q. Zhao, X. M. Wang, H. Y. Ma, *Transition Met. Chem.*, 2021, **46**, 335.

Table S3. Some weak interactions (Å) in the structures including convenient H-bonds, Weak CH…O H-bonds, anion-pi and pi/pi interactions.

Compound **1**

O(17)...H(26)	2.646	O(26)...H(23)	2.698
O(29)...H(24)	2.676	O(19)...H(2)	2.686
C(4)-H(4)...O(13)	2.467	C(2)-H(2B)...O(13)	2.654
C(15)-H(15)...O(39)	2.656	C(23)-H(23)...O(29)	2.472

C(2)...O(19)	3.157	C(17)...O(19)	3.123
C(23)...O(3)	3.179	C(2)...O(13)	3.282
		Compound **2**	
O(26)...H(63A)	2.700	O(54)...H(63B)	2.658
O(10)...H(33A)	2.570	O(56)...H(33B)	2.501
C(15)-H(15)...O(62)	2.704	C(20)-H(20)...O(24)	2.719
C(25)-H(25)...O(4)	2.503	C(6)-H(6)...O(46)	2.424
C(1)...O(5)	3.043	C(6)...O(5)	3.001
C(6)...O(46)	3.213	C(21)...O(17)	3.055
N(2)-H(2)...O31	1.791	N(3)-H(3)...O38	2.137
N(5)-H(5B)...O63	1.845	N(11)-H(11)...O2	1.818
		Compound **3**	
O(11)...H(41B)	2.361	O(36)...H(46B)	2.581
O(24)...H(46A)	2.461	O(35)...H(45B)	2.438
C(13)-H(13B)...O(13)	2.407	C(2)-H(2)...O(22)	2.615
C(6)-H(6)...O(41)	2.648	C(24)-H(24)...O(29)	2.679
C(24)...O(32)	3.211	C(22)...O(27)	3.133
C(17)...O(35)	3.134	C(26)...O(29)	3.177
		Compound **4**	
O(33)...H(41A)	2.193	C(16)-H(16)...O(40)	2.485
C(20)-H(20)...O(34)	2.499	C(24)-H(24)...O(36)	2.389
C(23)-H(23)...O(32)	2.646	C(3)-H(3)...O(37)	2.697
C(4)...O(26)	3.050	C(4)...O(26)	3.061
C(1)...O(11)	3.070	C(7)...O(29)	3.216
		Compound **5**	
O(9)...H(4WB)	2.013	O(10)...H(4WA)	2.039
O(11)...H(1WA)	2.138	O(2W)...H(1WA)	2.158
C(13)-H(13)...O(7)	2.639	C(10)-H(10)...O(8)	2.401
C(11)-H(11)...O(6)	2.355	C(12)-H(12)...O(3)	2.421
C(7)...O(1)	3.212	C(12)...O(7)	3.187
C(13)...O(7)	3.090	C(12)...O(1W)	2.961
		Compound **6**	
O(33)...H(8B)	2.153	O(4)...H(38B)	1.982
O(36)...H(38A)	1.957	O(12)...H(40A)	2.112
C(7)-H(7)...O(38)	2.556	C(3)-H(3)...O(3)	2.557
C(6)-H(6)...O(37)	2.158	N(2)-H(2)...O(13)	2.027
C(7)...O(12)	3.156	C(9)...O(23)	3.210
C(6)...O(37)	3.049	C(3)...O(3)	3.370
		Compound **7**	
O(25)...H(7A)	2.229	O(31)...H(7B)	2.184
O(29)...H(27B)	2.177	O(5)...H(13B)	2.221
C(8)-H(8)...O(10)	2.475	C(8)-H(8)...O(2)	2.693
C(12)-H(12)...O(5)	2.690	C(6)-H(6)...O(21)	2.623
C(12)...O(13)	3.146	C(4)...O(7)	3.148

C(1)...O(7)	2.967	C(6)...O(19)	2.871

The frames collected were intergated and scaled with APEX3. Non hydrogen atoms are directly determined by SHELXT, including free solvent molecules. The O atoms on some POM anions have been disorderly refined. The occupancy of some free solvent molecules was refined to make its temperature factor reasonable. All the hydrogen atoms attached to carbon atoms were generated geometrically. The H atoms on O and N were identified from the Q-peak diagram with combination of hydrogen bonds.

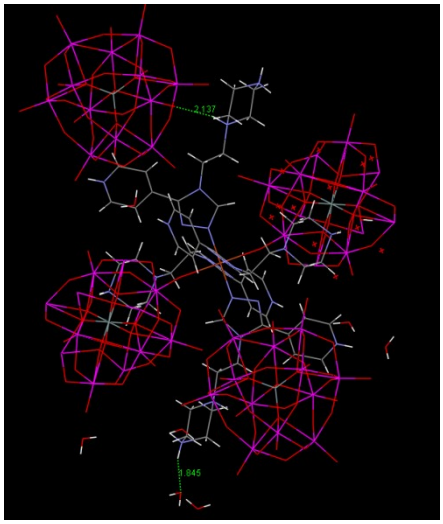

Fig. S1. The N-H…O bonds in compound **2**.

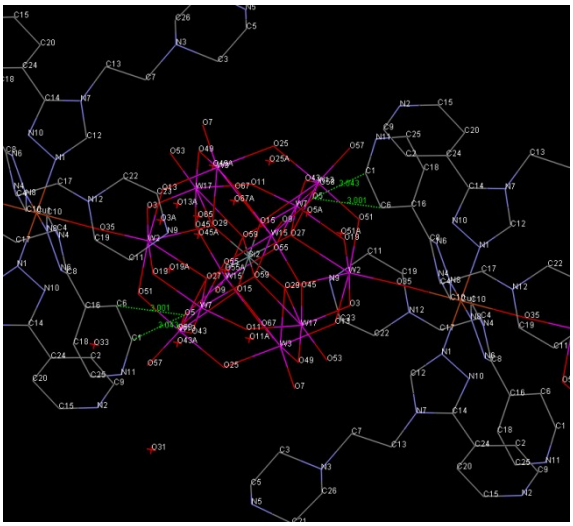

Fig. S2. The anion-pi interactions in the structure between pyridyl rings and POM anions in compound **2**, such as C1...O5 = 3.043 Å and C6...O5 = 3.001 Å.

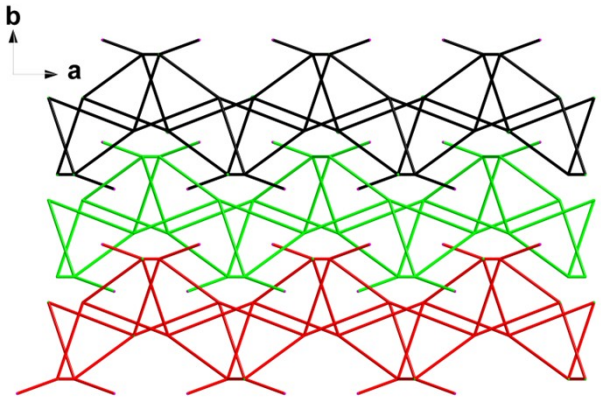

Fig. S3. Adjacent layers arranging in parallel of compound **3**.

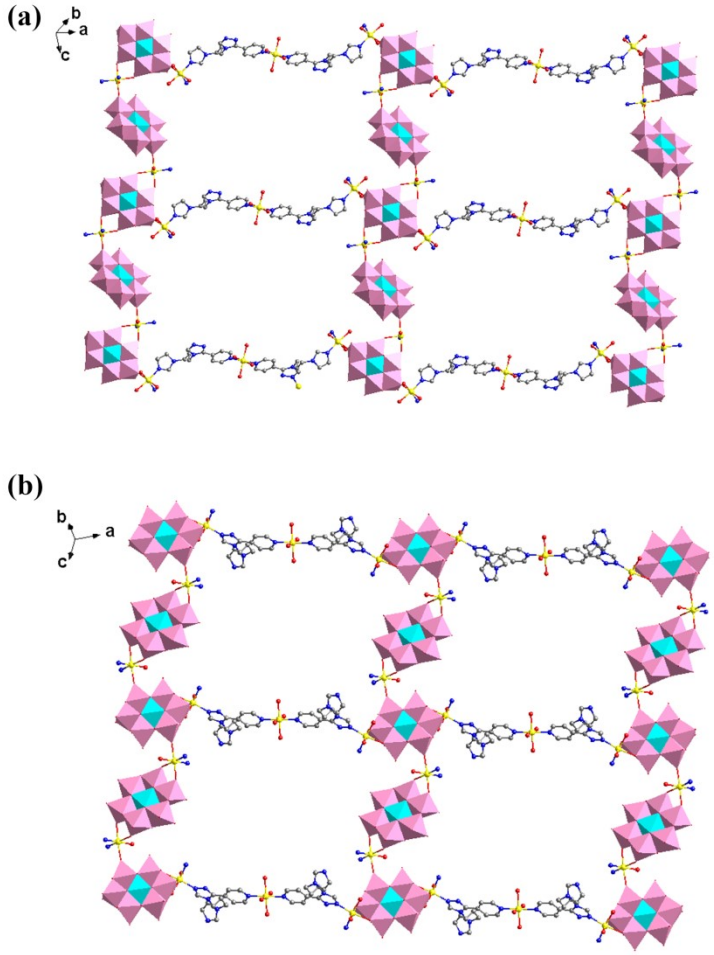

Fig. S4. Two kinds of layers in 3D framework of compound **5** viewing along different directions.

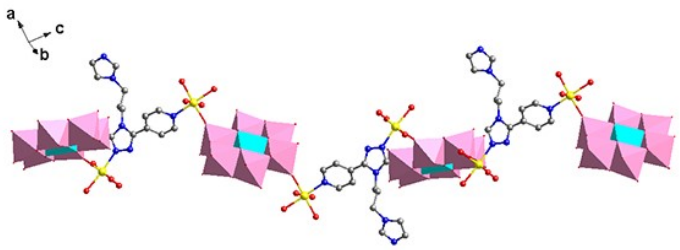

Fig. S5. (a) The 1D chain of **6** with $[Co_2(Ptpi)]^{4+}$ subunits linked by $TeMo_6$ anions. (b) the 2D layer of compound **6**.

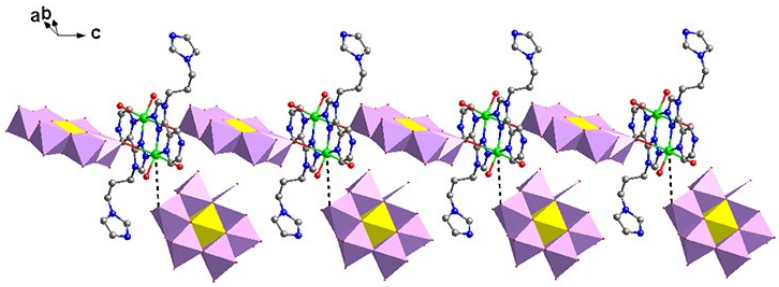

Fig. S6. The 1D chain of compound **7** with the $TeMo_6$ anions linked by $[Cu_2(Ztpi)_2(H_2O)_4]^{4+}$ subunits.

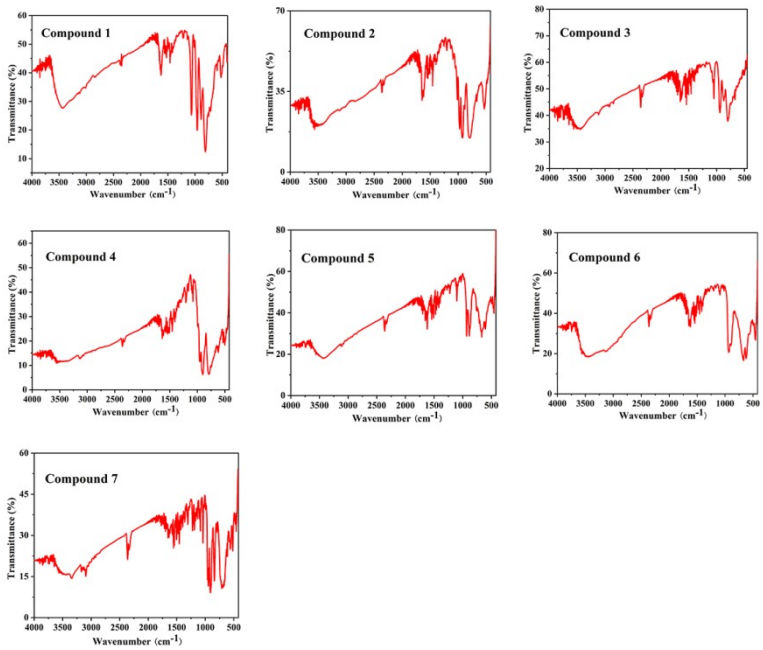

Fig. S7. The IR spectra of compounds **1**–**7**.

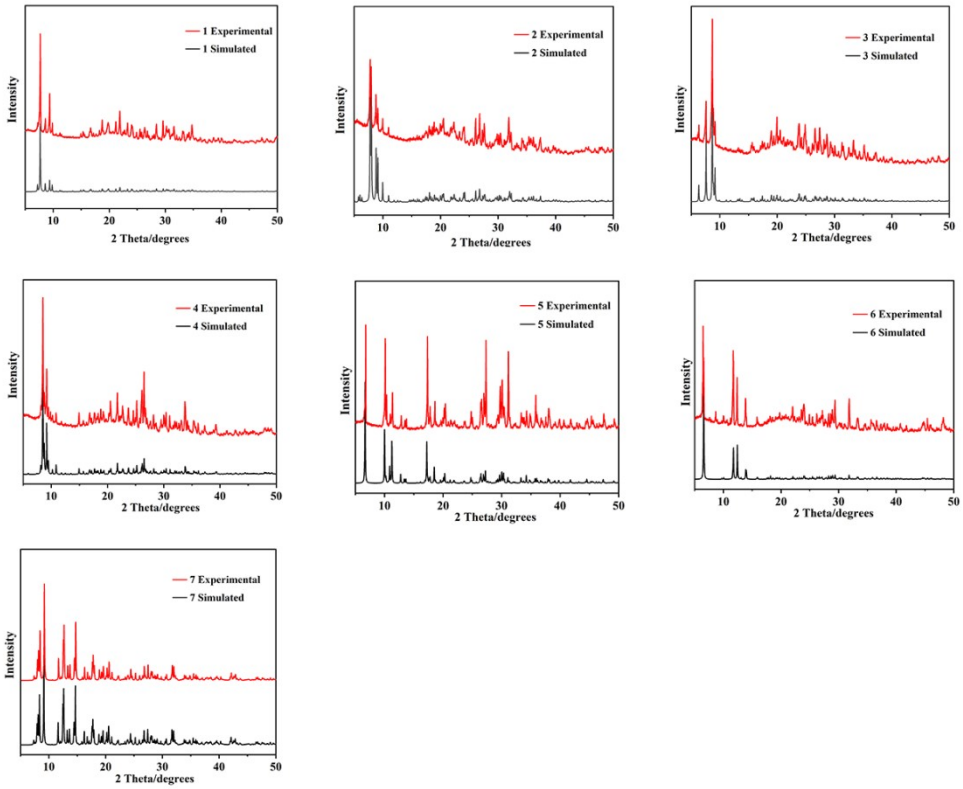

Fig. S8. The PXRD spectra of compounds **1–7**.

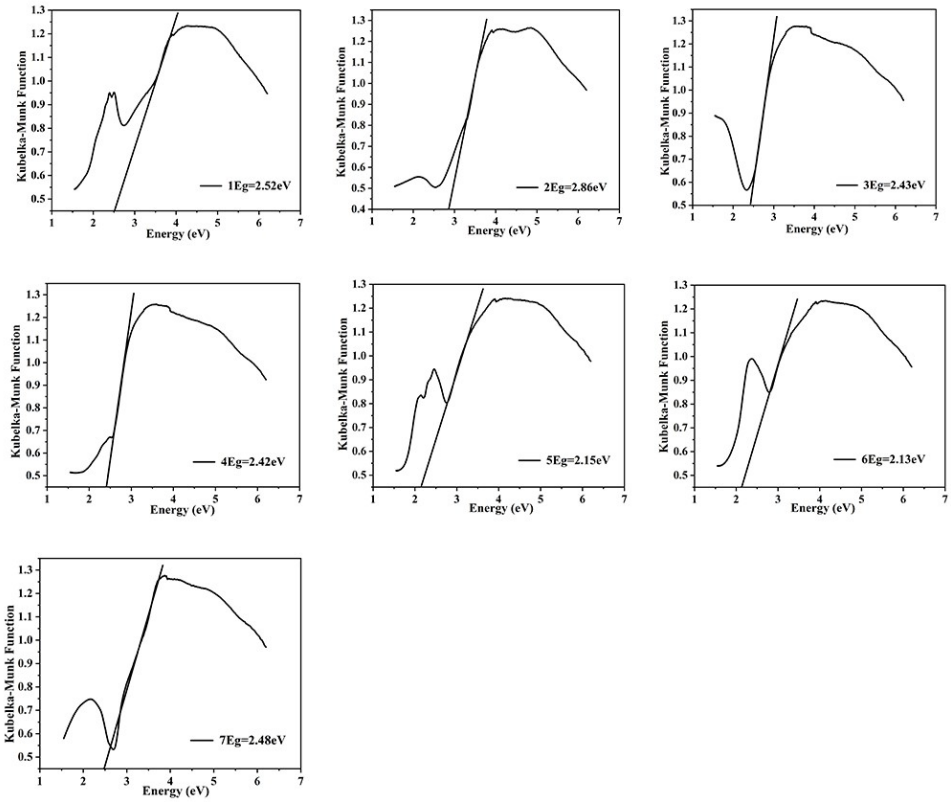

Fig. S9. The solid-state optical diffuse-reflectance spectra of compounds **1–7**.

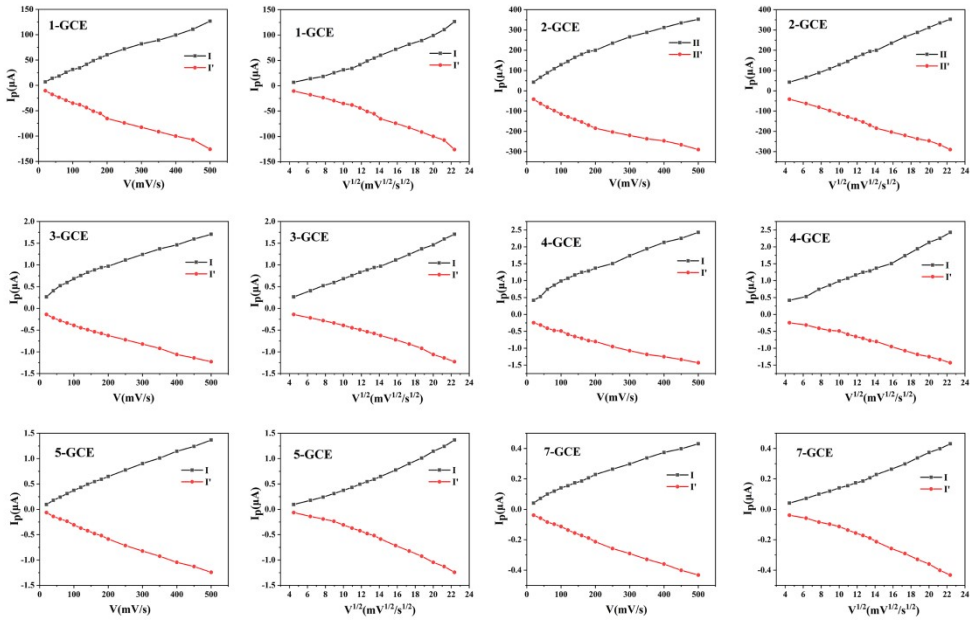

Fig. S10. The dependence of anodic peak and cathodic peak currents of **n**–GCEs (n = **1**, **2**, **3**, **4**, **5**, **7**) on scan rates.

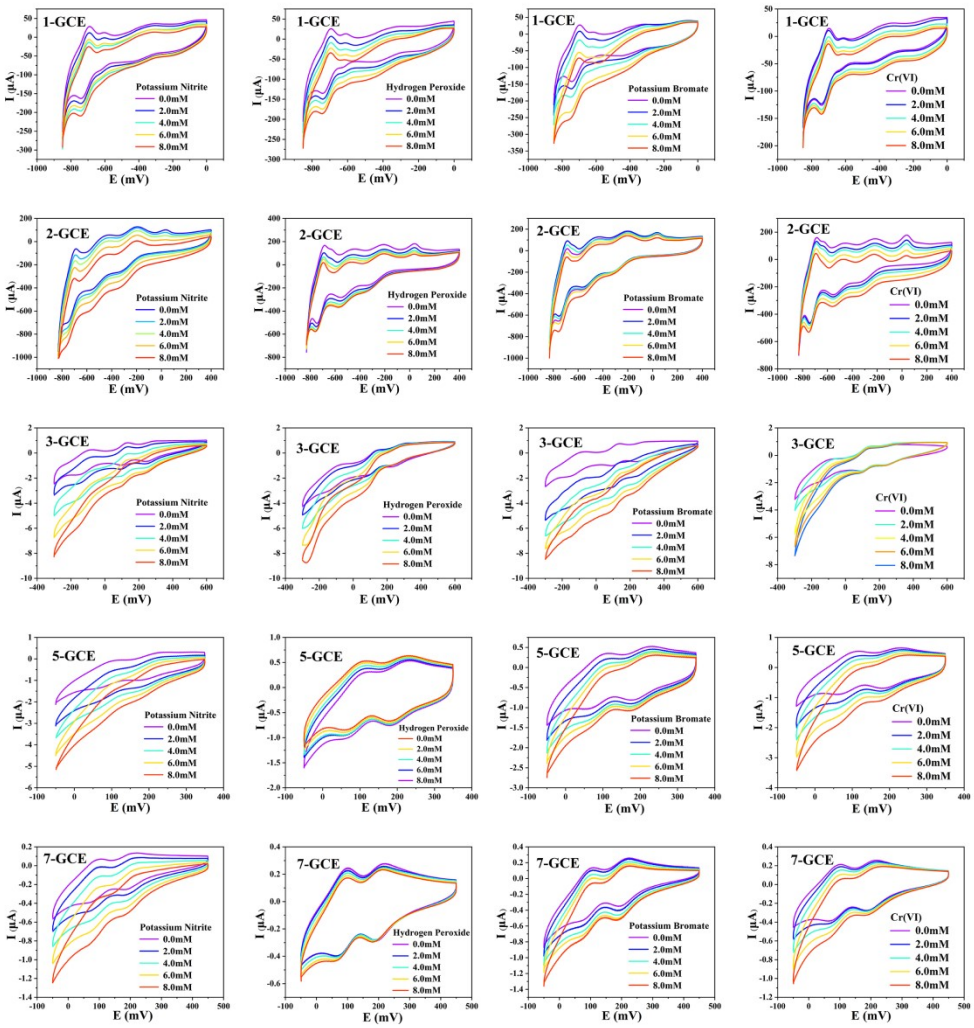

Fig. S11. Cyclic voltammograms of the **n–**GCEs (n = **1**, **2**, **3**, **5** and **7**) in 0.1 M H_2SO_4 + 0.5 M Na_2SO_4 aqueous solution containing 0–8 mM $KNO_2/H_2O_2/KBrO_3/Cr^{6+}$. Scan rate: 200 mV·s^{-1}.

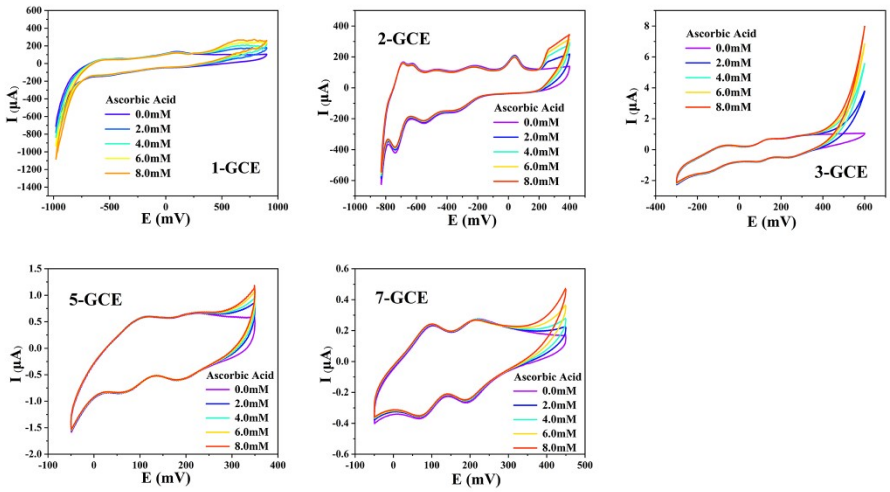

Fig. S12. Cyclic voltammograms of the **n–**GCEs (n = **1**, **2**, **3**, **5** and **7**) in 0.1 M H_2SO_4 + 0.5 M Na_2SO_4 aqueous solution containing 0–8 mM AA. Scan rate: 200 $mV \cdot s^{-1}$.

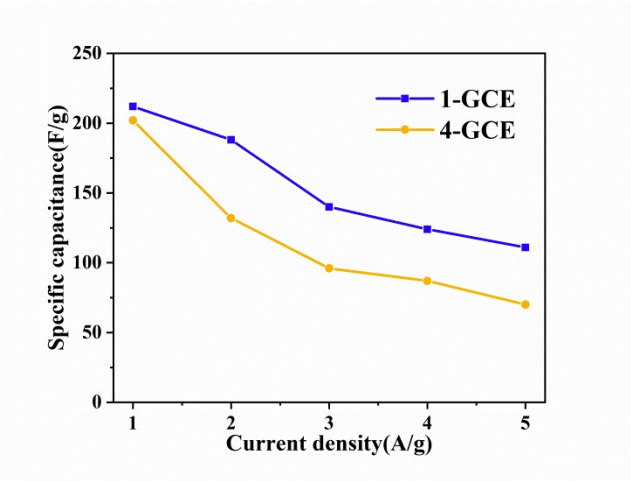

Fig. S13. The comparison of specific capacitance between **1–**GCE and **4–**GCE at different current densities.

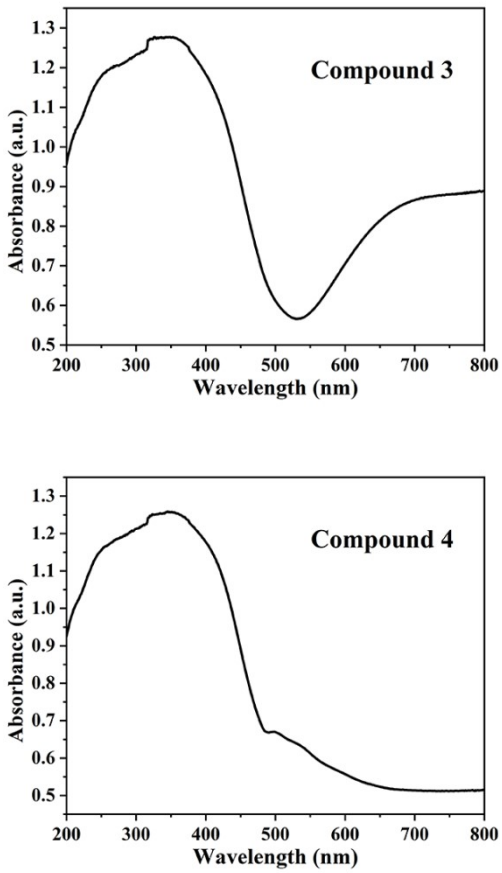

Fig. S14. The solid-state UV-vis diffuse reflection spectra of compounds **3** and **4**.

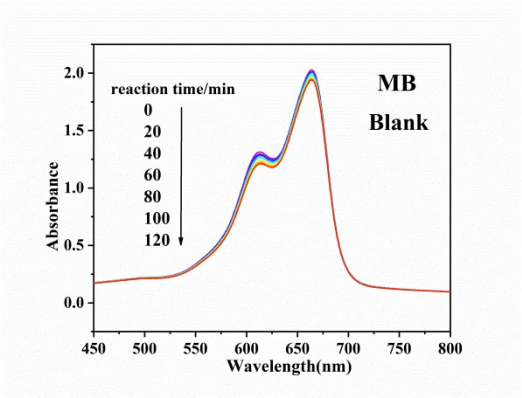

Fig. S15. UV spectra of the MB solution without compounds used as the photocatalytic catalysts.

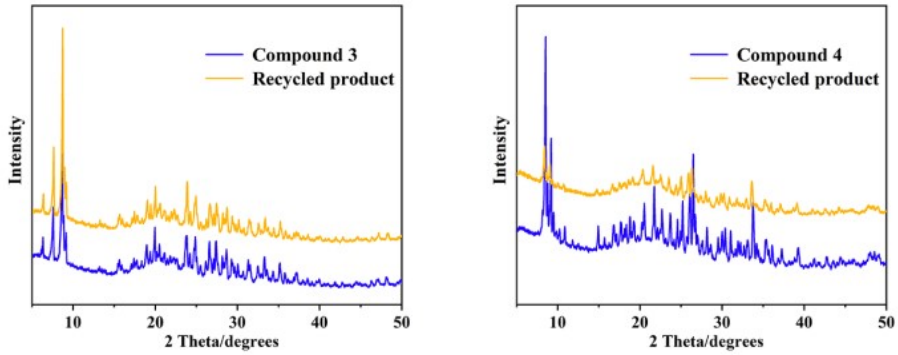

Fig. S16. The PXRD patterns of compounds **3** and **4** before and after the photoelectrocatalytic reaction.